Available online at www.sciencedirect.com

SciVerse ScienceDirect

Journal of the European Ceramic Society 32 (2012) 433–439

www.elsevier.com/locate/jeurceramsoc

Phase diagram and properties of $Pb(In_{1/2}Nb_{1/2})O_3$–$Pb(Mg_{1/3}Nb_{2/3})O_3$–$PbTiO_3$ polycrystalline ceramics

Dawei Wang [a,b], Maosheng Cao [a,**], Shujun Zhang [b,*]

[a] School of Materials Science and Engineering, Beijing Institute of Technology, Beijing 100081, China
[b] Materials Research Institute, Pennsylvania State University, University Park, PA 16802, USA

Received 21 July 2011; received in revised form 8 August 2011; accepted 11 August 2011
Available online 3 September 2011

Abstract

yPb($In_{1/2}Nb_{1/2}$)O_3–$(1-x-y)$Pb($Mg_{1/3}Nb_{2/3}$)O_3–xPbTiO$_3$ (yPIN–$(1-x-y)$PMN–xPT) polycrystalline ceramics with morphotropic phase boundary (MPB) compositions were synthesized using columbite precursor method. X-ray diffraction results indicated that the MPB of PIN–PMN–PT was located around PT = 0.33–0.36, confirmed by their respective dielectric, piezoelectric and electromechanical properties. The optimum properties were found for the MPB composition 0.36PIN–0.30PMN–0.34PT, with dielectric permittivity ε_r of 2970, piezoelectric coefficient d_{33} of 450 pC/N, planar electromechanical coupling k_p of 49%, remanent polarization P_r of 31.6 μC/cm^2 and T_C of 245 °C. According to the results of dielectric and pyroelectric measurements, the Curie temperature T_C and rhombohedral to tetragonal phase transition temperature T_{R-T} were obtained, and the "flat" MPB for PIN–PMN–PT was achieved, indicating that the strongly curved MPB in PMN–PT system was improved by adding PIN component, offering the possibility to grow single crystals with high electromechanical properties and expanded temperature usage range (limited by T_{R-T}).

Keywords: Sintering; Dielectric properties; Piezoelectric properties; Ferroelectric properties; PIN–PMN–PT

1. Introduction

Relaxor-$PbTiO_3$ (PT) based single crystals, such as $Pb(Mg_{1/3}Nb_{2/3})O_3$–$PbTiO_3$ (PMN–PT) and $Pb(Zn_{1/3}Nb_{2/3})O_3$–$PbTiO_3$ (PZN–PT), were found to possess extra high electromechanical coupling factor ($k_{33} > 0.9$) and piezoelectric coefficient ($d_{33} > 1500$ pC/N) that far out perform polycrystalline PZT-based ceramics (k_{33} ~0.7 and d_{33} ~400–600 pC/N), making them promising candidates for medical ultrasonic imaging, sonar transducers, and solid-state actuators.[1–3] Although relaxor-PT based single crystals have excellent piezoelectric and electromechanical properties, their relatively low Curie temperature (T_C ~130–170 °C) becomes a critical limitation for applications, where the thermal stability is required, in terms of dielectric and piezoelectric property variations and depolarization as a result of post-fabrication process in transducers.[3] Their usage temperature ranges are further restricted by ferroelectric rhombohedral to ferroelectric tetragonal phase transition (T_{R-T} ~60–95 °C), occurring at significantly lower temperatures due to the strongly curved morphotropic phase boundary (MPB).[3–5]

A broader temperature operating range would allow for greater device design flexibility and therefore a wider range of potential applications. Thus, new piezoelectric single crystal compositions, which will be able to operate at higher temperature than current state-of-the-art PMN–PT/PZN–PT single crystals, are desirable.[6] In order to find the possibility of single crystals for the next generation of transduction devices, numerous studies are focused on exploring new high performance ferroelectric systems with higher T_C/T_{R-T} over the past few years.[7–10]

Perovskite $Pb(In_{1/2}Nb_{1/2})O_3$ (PIN) is a typical relaxor ferroelectric material with a T_C of about 90 °C. The solid solution of the PIN–PT binary system exhibits a MPB near 37 mol% PT, where high piezoelectric and dielectric properties can be obtained. The Curie temperature of PIN–PT

* Corresponding author.
** Corresponding author.
E-mail addresses: caomaosheng@bit.edu.cn (M. Cao), soz1@psu.edu (S. Zhang).

0955-2219/$ – see front matter © 2011 Elsevier Ltd. All rights reserved.
doi:10.1016/j.jeurceramsoc.2011.08.025

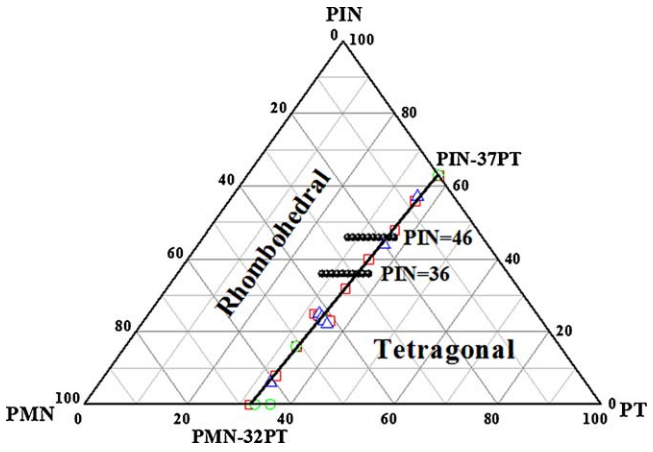

Fig. 1. Phase diagram of PIN–PMN–PT ternary system. Black dots are the selected compositions in this work. Other data is from the published papers (Red hollow squares: Hosona et al.[11]; Blue hollow triangles: Lin et al.[15]; Green hollow circles: Pham-Thi, et al.[16]). (For interpretation of the references to color in this figure legend, the reader is referred to the web version of the article.)

with MPB composition is about 320 °C, much higher than that of PMN–PT.[11] Consequently, it is promising to improve the T_C/T_{R-T} of PMN–PT system by adding PIN component. Recently, the new relaxor-PT based ternary single crystal system $Pb(In_{1/2}Nb_{1/2})O_3$–$Pb(Mg_{1/3}Nb_{2/3})O_3$–$PbTiO_3$ (PIN–PMN–PT) was reported to possess higher $T_C > 170$ °C and $T_{R-T} > 120$ °C, and comparable piezoelectric properties to the binary crystal systems PMN–PT, indicating that PIN–PMN–PT crystals are promising candidates for electromechanical devices where high temperature usage and thermal stability are required.[12–14] However, studies of PIN–PMN–PT system have been focused on the PIN in the range of 0.23–0.35, with T_{R-T} less than 135 °C, T_C/T_{R-T} of PIN–PMN–PT are needed to be further improved to satisfy practical applications for higher temperature

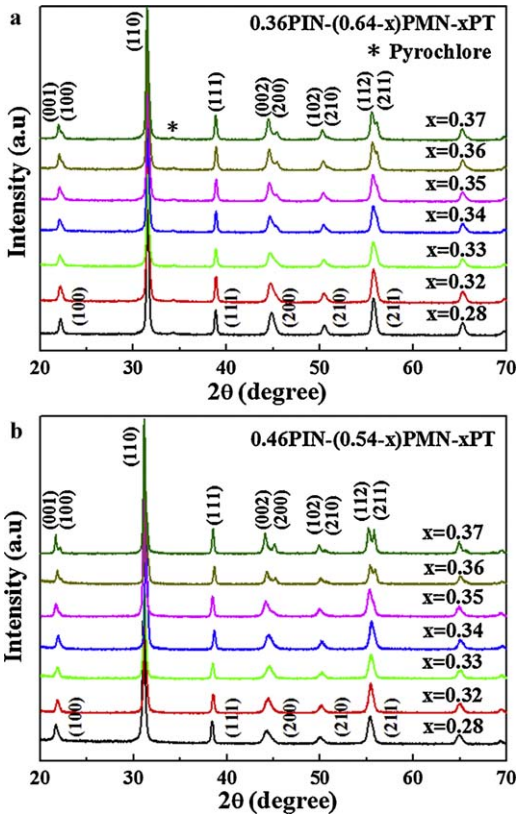

Fig. 2. XRD patterns of (a) 0.36PIN–$(0.64-x)$PMN–xPT and (b) 0.46PIN–$(0.54-x)$PMN–xPT. The space groups were determined to be P4 mm and R3c for tetragonal and rhombohedral phases, respectively, according to the XRD patterns.

range. Thus, it is necessary to investigate the PIN–PMN–PT ternary system with higher PIN content level.

In this work, in order to obtain higher T_C/T_{R-T} in PIN–PMN–PT ternary system, PIN–PMN–PT ceramics with

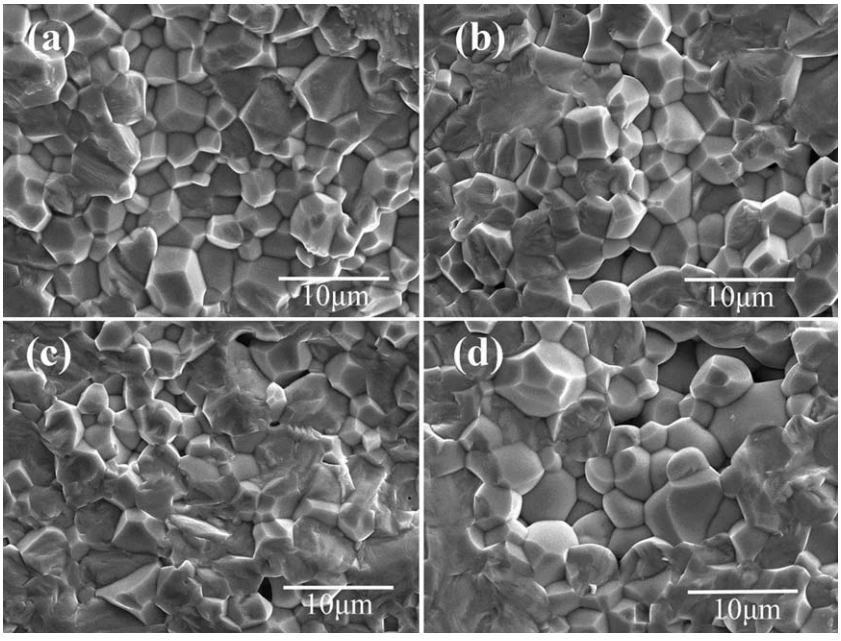

Fig. 3. SEM micrographs of the fracture surface for 0.46PIN–$(0.54-x)$PMN–xPT: (a) $x = 0.33$; (b) $x = 0.34$; (c) $x = 0.35$; (d) $x = 0.36$.

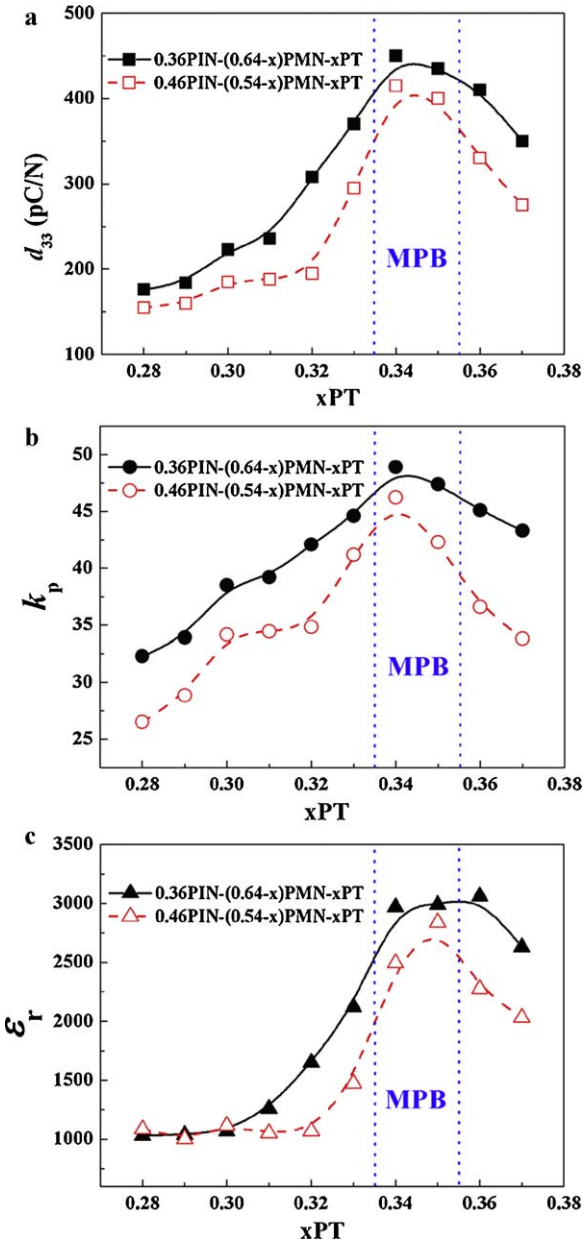

Fig. 4. The piezoelectric and dielectric properties of yPIN–$(1-x-y)$PMN–xPT as a function of PT: (a) piezoelectric coefficient d_{33}; (b) planar electromechanical coupling k_p and (c) dielectric permittivity ε_r.

high PIN content were synthesized using columbite precursor method. Dielectric- and pyroelectric-temperature measurements were used to determine the T_C/T_{R-T}. Phase structure, dielectric, piezoelectric and ferroelectric properties of PIN–PMN–PT ceramics were studied in detail.

2. Experimental

The PIN–PMN–PT ternary ceramics with compositions of yPb$(In_{1/2}Nb_{1/2})O_3$–$(1-x-y)$Pb$(Mg_{1/3}Nb_{2/3})O_3$–xPbTiO$_3$ (yPIN–$(1-x-y)$PMN–xPT, $x=0.28$–0.37 and $y=0.36$, 0.46) were prepared using two-step columbite precursor

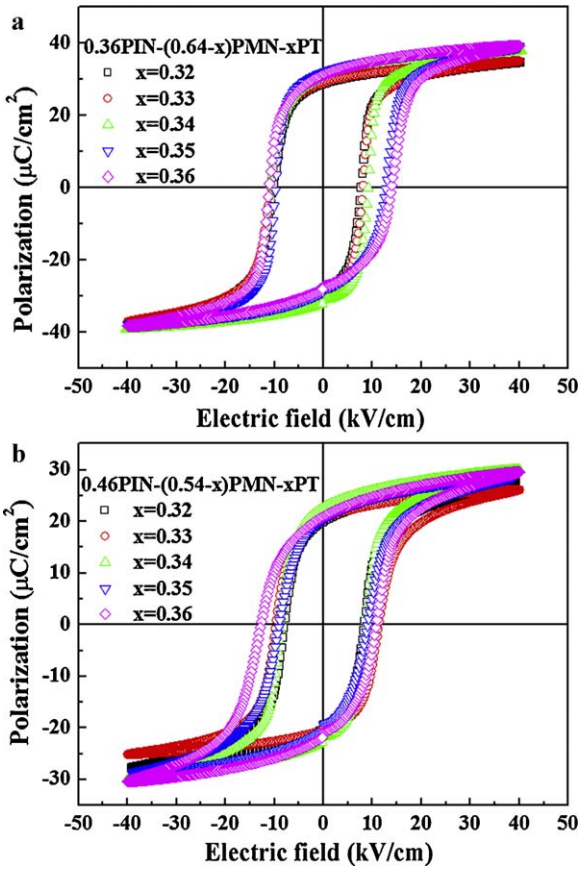

Fig. 5. The ferroelectric hysteresis of (a) 0.36PIN–$(0.64-x)$PMN–xPT; (b) 0.46PIN–$(0.54-x)$PMN–xPT.

method.[11,15–17] The studied compositions are shown in Fig. 1. Raw materials of $MgCO_3$ (99.9%, Alfa Aesar, Ward Hill, MA), Nb_2O_5 (99.9%, Alfa Aesar) and In_2O_3 (99.9%, Alfa Aesar) were used to synthesize columbite precursors of $MgNb_2O_6$ and $InNbO_4$ at 1000 °C and 1100 °C, respectively. Pb_3O_4 (99%, Alfa Aesar), TiO_2 (99.9%, Ishihara, San Francisco, CA), $MgNb_2O_6$ and $InNbO_4$ powders were batched stoichiometrically according to the nominal compositions and wet-milling in alcohol for 24 h. The dried mixed powders were calcined at 800 °C for 4 h. The synthesized powders were subsequently vibratory milled in alcohol for 12 h. The powders were granulated and pressed into pellets with 12 mm in diameter. Following binder burnout at 550 °C, the pellets were sintered in a sealed crucible at 1220–1280 °C, where $PbZrO_3$ was used as lead source to minimize PbO evaporation.

The density of the sintered samples was measured using the Archimedes method. The phase and morphologies of the sintered samples were determined using X-ray powder diffraction (XRD, PADV and X2 diffractometers, Scintag, Cupertino, CA) and scanning electron microscope (SEM, Hitachi S-3500 N, Japan). For electrical test, plane-parallel plates of sintered samples were polished using 15 μm SiC powder. Silver paste was printed to form electrodes on both sides of the disc samples and then fired at 700 °C for 10 min. Poling was carried out in silicon oil at 120 °C for 10 min with an electric field of 30 kV/cm. Dielectric measurements were carried out on poled samples using a

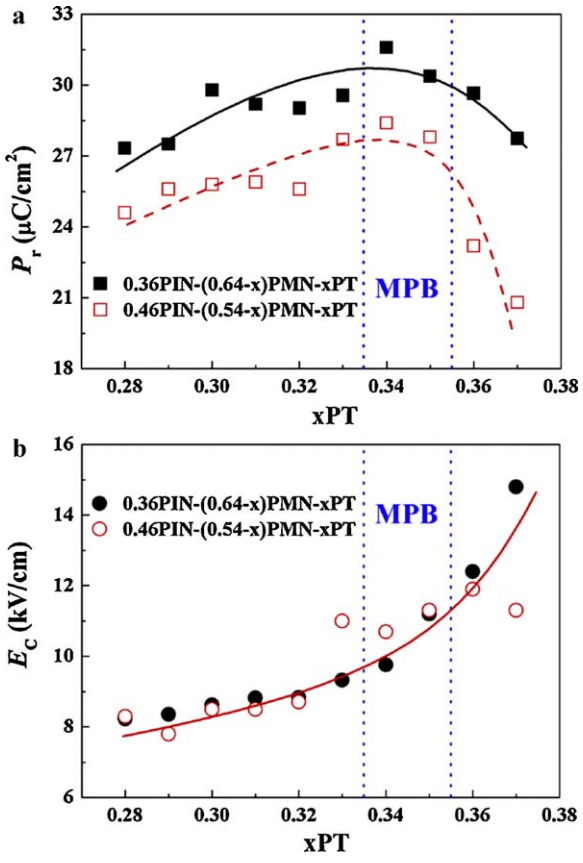

Fig. 6. (a) Remanent polarization P_r and (b) coercive field E_C of yPIN–$(1-x-y)$PMN–xPT as a function of PT.

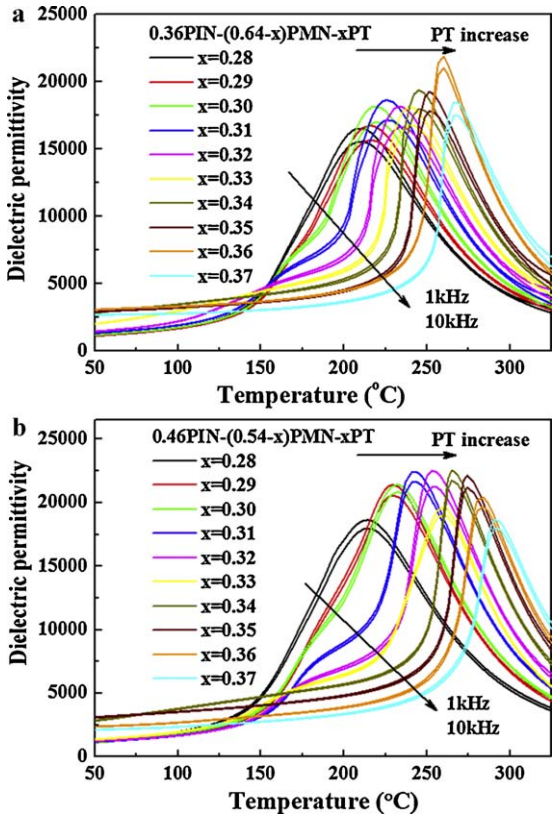

Fig. 7. The temperature dependence of dielectric permittivity for (a) 0.36PIN–$(0.64-x)$PMN–xPT and (b) 0.46PIN–$(0.54-x)$PMN–xPT.

multi-frequency precision LCRF meter (HP 4184A, Hewlett Packard, Palo Alto, CA). Piezoelectric coefficients were measured on disk samples using a Berlincourt d_{33} meter (ZJ-2, Institute of Acoustics Academia Sinica, Beijing, China). Polarization hysteresis and strain-electric field behavior were determined using a modified Sawyer–Tower circuit driven by a lock-in amplifier (Model SR830, Stanford Research System, Sunnyvale, CA) at a frequency of 1 Hz. The planar electromechanical coupling k_p and mechanical quality factor Q_m were determined from the resonance and antiresonance frequencies, which were measured using an Impedance/Gain-phase analyzer (HP 4194A, Hewlett-Packard, Palo Alto, CA), according to IEEE standards.[18,19] The pyroelectric property was measured by the static Byer–Roundy method[20] and a picoammeter (HP 4140B, Hewlett Packard, Palo Alto, CA) was used to measure the pyroelectric current.

3. Results and discussion

XRD patterns of the studied compositions for yPIN–$(1-x-y)$PMN–xPT are shown in Fig. 2. All the samples were found to be pure perovskite except the compositions with 0.36PIN, where small peaks of pyrochlore phase were indicated in Fig. 2(a). The typical tetragonal phase symmetry for perovskite at room temperature is characterized by (2 0 0) peak splitting around $2\theta = 45^\circ$, which was used to determine the MPB compositions, separating rhombohedral and tetragonal phases.[21,22] It was found that with increasing PT content, the (2 0 0) peak gradually split, indicating the phase transition from rhombohedral phase to tetragonal phase. As a result, the compositions with PT content of 0.33, 0.34 and 0.35 for 0.36PIN–$(0.64-x)$PMN–xPT and 0.34, 0.35 and 0.36 for 0.46PIN–$(0.54-x)$PMN–xPT belong to the MPB region according to the XRD patterns.

SEM micrographs of the fracture surface for 0.46PIN–$(0.54-x)$PMN–xPT with different PT contents are shown in Fig. 3. It was clearly observed that all samples were highly dense, with a mixture of transgranular and intergranular characteristics.[23] With increasing PT content, the grain size changed slightly, which was found to be on the order of 2–5 μm.

The piezoelectric and dielectric properties of yPIN–$(1-x-y)$PMN–xPT with different PT contents are shown in Fig. 4. It was found that the piezoelectric coefficient d_{33}, planar electromechanical coupling k_p and dielectric permittivity ε_r reached the maxima in the range of PT = 0.33–0.36, which is attributed to the enhanced polarizability for MPB compositions.

The ferroelectric hysteresis of yPIN–$(1-x-y)$PMN–xPT with different PT contents is shown in Fig. 5. The corresponding remanent polarization P_r and coercive field E_C as a function of PT are shown in Fig. 6. It was observed that with increasing PT content from 0.28 to 0.36, P_r increased firstly, reaching

Table 1
Piezoelectric, dielectric and ferroelectric properties of 0.36PIN–(0.64 − x)PMN–xPT.

Composition (PIN–PMN–PT)	Density (g/cm^3)	d_{33} (pC/N)	k_p (%)	Q_m	ε_r	tanδ (%)	T_C (°C)	T_{R-T} (°C)	P_r (μC/cm^2)	E_C (kV/cm)
36/36/28	8.2	180	32.3	260	1030	1	210	166	27.3	8.2
36/35/29	8.2	180	33.9	270	1040	0.9	215	163	27.5	8.4
36/34/30	8.2	220	38.5	240	1070	1	218	159	29.8	8.6
36/33/31	8.2	240	39.2	230	1260	0.9	225	163	29.2	8.8
36/32/32	8.2	310	42.1	200	1650	1	233	156	29.1	8.8
36/31/33	8.1	370	44.6	170	2120	1	239	158	29.6	9.3
36/30/34	8.1	450	49.0	130	2970	1.1	245	/	31.6	9.8
36/29/35	8.1	440	47.4	150	2990	1	251	/	30.4	11.2
36/28/36	8.0	410	45.1	150	3060	1	260	/	29.7	12.4
36/27/37	8.1	350	43.3	200	2630	0.7	266	/	27.7	14.8

d_{33}, piezoelectric coefficient; k_p, planar electromechanical coupling; Q_m, mechanical quality factor; ε_r, dielectric permittivity; tanδ, dielectric loss; T_C, Curie temperature; T_{R-T}, rhombohedral to tetragonal phase transition temperature; P_r, remanent polarization; E_C, coercive field.

Table 2
Piezoelectric, dielectric and ferroelectric properties of 0.46PIN–(0.54 − x)PMN–xPT.

Composition (PIN–PMN–PT)	Density (g/cm^3)	d_{33} (pC/N)	k_p (%)	Q_m	ε_r	tanδ (%)	T_C (°C)	T_{R-T} (°C)	P_r (μC/cm^2)	E_C (kV/cm)
46/26/28	8.2	160	26.5	240	1100	2.2	215	173	24.6	8.3
46/25/29	8.1	160	28.9	220	1000	2.2	229	174	25.6	7.8
46/24/30	8.1	190	34.1	210	1110	2.3	232	177	25.8	8.5
46/23/31	8.2	190	34.5	180	1050	2.1	242	174	25.9	8.5
46/22/32	8.3	200	34.8	180	1070	1.8	253	164	25.6	8.7
46/21/33	8.1	300	41.2	180	1470	1.8	260	158	27.7	11.2
46/20/34	8.2	420	46.2	120	2490	1.7	265	158	28.4	10.7
46/19/35	8.2	400	42.3	110	2840	1.5	274	/	27.8	11.3
46/18/36	8.1	330	36.6	130	2270	1.4	284	/	23.2	11.9
46/17/37	8.1	280	33.8	150	2030	1.2	291	/	20.8	11.3

the maxima at PT = 0.34, above which, P_r decreased. Due to the coexistence of ferroelectric rhombohedral and tetragonal phases in the MPB compositions of yPIN–(1 − x − y)PMN–xPT, the optimum domain reorientation during poling can be achieved, leading to the enhanced P_r for MPB composition. Coercive field E_C, however, was found to increase monotonously with increasing PT content, as shown in Fig. 6(b), indicating that the domain switching becomes harder, attributed to the increase of the tetragonal phase.

The temperature dependence of the dielectric permittivity for yPIN–(1 − x − y)PMN–xPT is shown in Fig. 7. In most cases, two dielectric anomalies can be observed, corresponding to the rhombohedral to tetragonal phase transition temperature T_{R-T} and Curie temperature T_C, respectively.

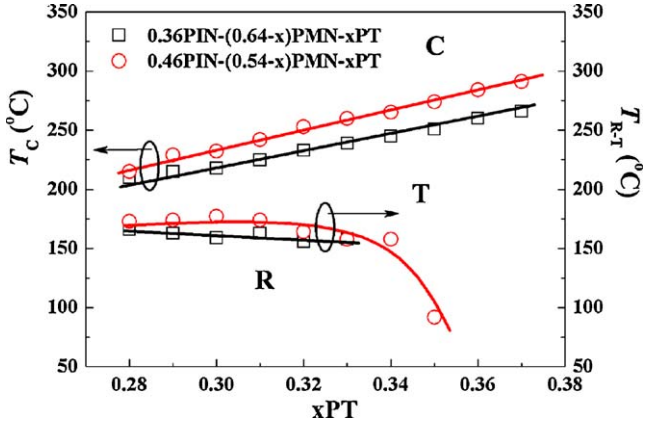

Fig. 8. Rhombohedral to tetragonal phase transition temperature T_{R-T} and Curie temperature T_C of PIN–PMN–PT as a function of PT (C, cubic phase; R, rhombohedral phase; T, tetragonal phase).

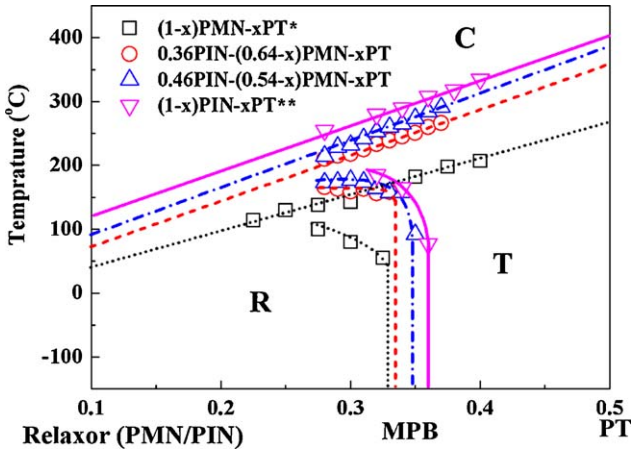

Fig. 9. The shape of MPB for the PIN–PMN–PT ternary system (*Choi et al.[24]; **Alberta[25]).

The values of T_C can be easily determined by the dielectric maxima, as shown in Fig. 7, while the values of T_{R-T} can be confirmed by the pyroelectric measurements.[24] Consequently, the T_C/T_{R-T} dependence as a function of PT was obtained and given in Fig. 8. It was clear that with increasing PT content, T_C increased from 166 °C to 266 °C and 215 °C to 291 °C for yPIN–$(1-x-y)$PMN–xPT with 0.36PIN and 0.46PIN, respectively, while, T_{R-T} changed slightly in a wide PT range. Of particular interest is that high $T_{R-T} > 170$ °C was achieved for 0.46PIN–$(0.54-x)$PMN–xPT, attractive for single crystal growth. Detailed piezoelectric, dielectric and ferroelectric properties for yPIN–$(1-x-y)$PMN–xPT with 0.36PIN and 0.46PIN are listed in Tables 1 and 2, respectively.

According to the data from dielectric and pyroelectric measurements in this work, including reported results,[24,25] the shape of MPB for the PIN–PMN–PT ternary system was obtained, as shown in Fig. 9. It is evident that with increasing PIN content, the T_C/T_{R-T} are improved greatly, due to the higher T_C of PIN (90 °C) than that of PMN (−10 °C).[11,24] Of particular significance is that the strongly curved MPB in PMN–PT system became almost "flat" in a broad range of PT content (0.28–0.34) for PIN–PMN–PT ternary system, due to the addition of PIN component, demonstrating that compositions with improved piezoelectric properties and broad temperature usage range are expected at MPB region, as shown in Figs. 8 and 9,[26] attractive for electromechanical applications with higher temperature usage range.

4. Conclusions

In conclusion, PIN–PMN–PT ternary ceramics with MPB compositions were prepared using two-step columbite precursor method. Phase structure, dielectric, piezoelectric and ferroelectric properties were investigated. The optimum properties were found for the MPB composition 0.36PIN–0.30PMN–0.34PT, with d_{33} of 450 pC/N, k_p of 49%, Q_m of 130, ε_r of 2970, tanδ of 1.1%, P_r of 31.6 μC/cm^2, E_C of 9.8 kV/cm and T_C of 245 °C. According to the dielectric- and pyroelectric-temperature measurements, the T_C/T_{R-T} were obtained as a function of PT, "flat" MPB in a broad PT range for the ternary PIN–PMN–PT system was achieved. It is significant that high T_{R-T} of 170–180 °C was achieved for PIN–PMN–PT ternary system, which is promising to grow high performance crystals with enhanced temperature usage range and thermal stability.

Acknowledgements

The authors thank Prof. Thomas R. Shrout for the helpful discussion. Authors from Beijing Institute of Technology acknowledge the National Natural Science Foundation of China under Grant Nos. 50742007, 50872159 and 50972014, and the National High Technology Research and Development Program of China under Grant No. 2007AA03Z103. The author (D.W. Wang) wishes to acknowledge the support from the China Scholarship Council. The work was supported by ONR.

References

1. Park SE, Shrout TR. Characteristics of relaxor-based piezoelectric single crystals for ultrasonic transducers. *IEEE Trans Ultrasonics Ferroelectr Frequency Control* 1997;**44**:1140–7.
2. Park SE, Shrout TR. Ultrahigh strain and piezoelectric behavior in relaxor based ferroelectric single crystals. *J Appl Phys* 1997;**82**:1804–11.
3. Zhang SJ, Shrout TR. Relaxor-PT single crystals: observations and developments. *IEEE Trans Ultrasonics Ferroelectr Frequency Control* 2010;**57**:2138–46.
4. Davis M, Damjanovic D, Setter N. Electric-field, temperature, and stress-induced phase transitions in relaxor ferroelectric single crystals. *Phys Rev B* 2006;**73**:014115.
5. Zhang SJ, Luo J, Xia R, Rehrig PW, Randall CA, Shrout TR. Field-induced piezoelectric response in $Pb(Mg_{1/3}Nb_{2/3})O_3$–$PbTiO_3$ single crystals. *Solid State Commun* 2006;**137**:16–20.
6. Zhang SJ, Luo J, Hackenberger W, Shrout TR. Characterization of $Pb(In_{1/2}Nb_{1/2})O_3$–$Pb(Mg_{1/3}Nb_{2/3})O_3$–$PbTiO_3$ ferroelectric crystal with enhanced phase transition temperatures. *J Appl Phys* 2008; **104**:064106.
7. Zhang SJ, Randall CA, Shrout TR. Characterization of perovskite piezoelectric single crystals of $0.43BiScO_3$–$0.57PbTiO_3$ with high Curie temperature. *J Appl Phys* 2004;**95**:4291.
8. Zhang SJ, Lebrun L, Rhee S, Eitel RE, Randall CA, Shrout TR. Crystal growth and characterization of new high Curie temperature $(1-x)BiScO_3$–$PbTiO_3$ single crystals. *J Cryst Growth* 2002;**236**: 210–6.
9. Xu GS, Chen K, Yang DF, Li J. Growth and electrical properties of large size PIN–PMN–PT crystals prepared by the vertical Bridgman technique. *Appl Phys Lett* 2007;**90**:032901.
10. Tian J, Han PD, Huang XL, Pan HX. Improved stability for piezoelectric crystals grown in the lead indium niobate–lead magnesium niobate–lead titanate system. *Appl Phys Lett* 2007;**91**:222903.
11. Hosona Y, Yamashita Y, Sakamoto H, Ichinose N. Dielectric and piezoelectric properties of $Pb(In_{1/2}Nb_{1/2})O_3$–$Pb(Mg_{1/3}Nb_{2/3})O_3$–$PbTiO_3$ ternary ceramic materials near the morphotropic phase boundary. *Jpn J Appl Phys* 2003;**42**:535–8.
12. Li F, Zhang SJ, Lin DB, Luo J, Xu Z, Wei XY, Shrout TR. Electromechanical properties of $Pb(In_{1/2}Nb_{1/2})O_3$–$Pb(Mg_{1/3}Nb_{2/3})O_3$–$PbTiO_3$ single crystals. *J Appl Phys* 2011;**109**:014108.
13. Li F, Zhang SJ, Xu Z, Wei XY, Luo J, Shrout TR. Electromechanical properties of tetragonal $Pb(In_{1/2}Nb_{1/2})O_3$–$Pb(Mg_{1/3}Nb_{2/3})O_3$–$PbTiO_3$ ferroelectric crystals. *J Appl Phys* 2010;**107**:054107.
14. Zhang SJ, Luo J, Hackenberger W, Sherlock NP, Meyer Jr RJ, Shrout TR. Electromechanical characterization of $Pb(In_{1/2}Nb_{1/2})O_3$–$Pb(Mg_{1/3}Nb_{2/3})O_3$–$PbTiO_3$ crystals as a function of crystallographic orientation and temperature. *J Appl Phys* 2009;**105**:104506.
15. Lin DB, Li ZR, Li F, Xu Z, Yao X. Characterization and piezoelectric thermal stability of PIN–PMN–PT ternary ceramics near the morphotropic phase boundary. *J Alloys Compd* 2010;**489**:115–8.
16. Pham-Thi M, Augier C, Dammak H, Gaucher P. Fine grains ceramics of PIN–PT, PIN–PMN–PT and PMN–PT systems: drift of the dielectric constant under high electric field. *Ultrasonics* 2006;**44**:e627–31.
17. Swartz SL, Shrout TR. Fabrication of perovskite lead magnesium niobate. *Mater Res Bull* 1982;**17**:1245–50.
18. IEEE standard on piezoelectricity, ANSI/IEEE Std. 176-1987. New York: IEEE; 1987.
19. Zhang SJ, Alberta EF, Eitel RE, Randall CA, Shrout TR. Elastic, piezoelectric, and dielectric characterization of modified $BiScO_3$–$PbTiO_3$ ceramics. *IEEE Trans Ultrasonics Ferroelectr Frequency Control* 2005; **52**:2131–9.
20. Byer RL, Roundy CR. Pyroelectric coefficient direct measurement technique and application to a nsec response time detector. *Ferroelectrics* 1972;**3**:333–8.
21. Yuan J, Wang DW, Lin HB, Zhao QL, Zhang DQ, Cao MS. Effect of ZnO whisker content on sinterability and fracture behaviour of PZT piezoelectric composites. *J Alloys Compd* 2010;**504**:123–8.

22. Hao H, Zhang SJ, Shrout TR. Dielectric and piezoelectric properties of the morphotropic phase boundary composition in the $(0.8-x)$ $Pb(Mg_{1/3}Ta_{2/3})O_3$–$0.2PbZrO_3$–$xPbTiO_3$ ternary system. *J Am Ceram Soc* 2008;**91**:2232–5.
23. Wang DW, Cao MS, Yuan J, Lu R, Li HB, Lin HB, Zhao QL, Zhang DQ. Effect of sintering temperature and time on densification, microstructure and properties of the PZT/ZnO nanowhisker piezoelectric composites. *J Alloys Compd* 2011;**509**:6980–6.
24. Choi SW, Shrout TR, Jang SJ, Bhalla AS. Dielectric and pyroelectric properties in the $Pb(Mg_{1/3}Nb_{2/3})O_3$–$PbTiO_3$ system. *Ferroelectrics* 1989;**100**:29–38.
25. Alberta EF. Relaxor based solid solution for piezoelectric and electrostrictive applications. Ph.D. Thesis, The Pennsylvania State University, 2003.
26. Li F, Zhang SJ, Xu_Z, Wei XY, Luo J, Shrout TR. Temperature independent shear piezoelectric response in relaxor-$PbTiO_3$ based crystals. *Appl Phys Lett* 2010;**97**:252903.